



**Title:**

**Shape Similarity Analysis and Standardization for Pre-bent Rod Design for Spinal Deformity Correction**

**Authors:**

Ayane Soutme, bvsb\_0410@eis.hokudai.ac.jp, Hokkaido University  
 Satoshi Kanai, kanai@ssi.ist.hokudai.ac.jp, Hokkaido University  
 Hiroaki Date, hdate@ssi.ist.hokudai.ac.jp, Hokkaido University  
 Hideki Sudo, hidekisudo@yahoo.co.jp, Hokkaido University  
 Terufumi Kokabu, m990015jp@yahoo.co.jp, Hokkaido University  
 Yuichiro Abe, menchi@athena.ocn.ne.jp, Eniwa Hospital  
 Hiroshi Moridaira, morihey@dokkyomed.ac.jp, Dokkyo Medical University  
 Hiroshi Taneichi, tane@dokkyomed.ac.jp, Dokkyo Medical University

**Keywords:**

Shape Similarity, Shape Standardization, Point Clouds, Triangle Mesh, Medial Axis, Pre-bent Spinal Rods, Spinal Deformity, Hierarchical Cluster Analysis, CT scan, Point Cloud Registration

**DOI:** 10.14733/cadconfP.2022.209-214

**Introduction:**

Spinal deformity is a disease in which the spinal column bends either toward the left, or right, and when it worsens deformity correction surgery is required. In surgery, two metal rods called “spinal rods” are bolted to the spinal column's left and right sides, as shown in Fig. 1(a) and 1(b). Currently, the orthodontic surgeons manually bend the rods during surgery to fit the corrective target shape suitable for each patient. However, this intraoperative rod bending work raises patient burden due to the increase in surgery time and the risk of rod breakage inside the body due to notched damages caused by bending work.

To solve the above-mentioned problem, the authors have proposed a surgical operation method for spinal deformity correction that uses a set of "pre-bent rods" [3], as shown in Fig. 1(c). The pre-bent rods consist of several standardized rods that have already been bent and deformed at the time of manufacture, and a rod that best suits a patient's spine is selected from the standardized rods during surgery. The method does not need any bending operation during the surgery and thus, can reduce the patient burden and risk of breakage. When designing pre-bent rods, it is essential to know the number of rods to be prepared and the kind of shapes required for the rods.

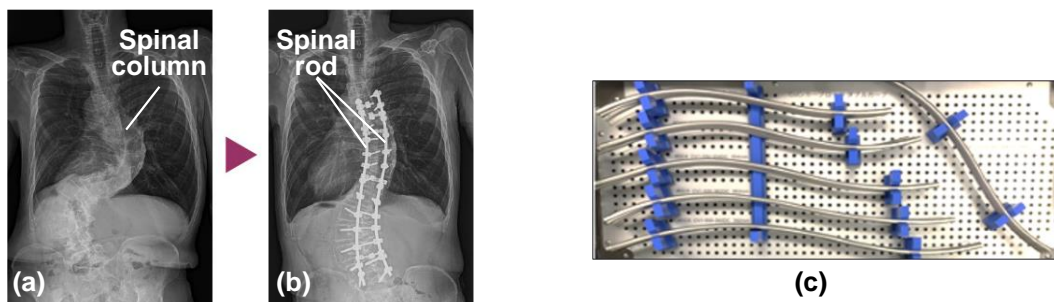


Fig. 1: (a) Spinal deformity, (b) Two spinal rods for deformity correction surgery, and (c) Examples of pre-bent rods for idiopathic scoliosis proposed in [3].

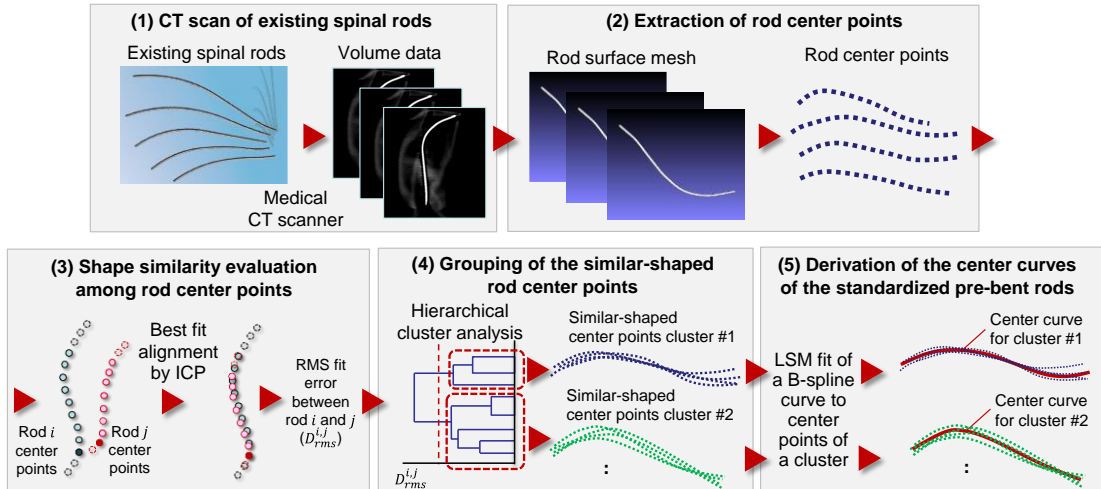


Fig. 2: Process pipeline of shape similarity analysis and standardization of pre-bent rods.

For designing the pre-bent rods for idiopathic scoliosis in [3], the authors have analyzed from an extensive collection of traced drawings the similarity in spinal rods of different shapes that are being used in current surgeries. They have shown that it is sufficient to prepare ten standardized rods with a planar curve shape [3]. On the other hand, the deformity in adult spinal has a greater degree than idiopathic scoliosis. Therefore, spinal rods designed with three-dimensional (3D) spatial curves are necessary for correction surgeries, and pre-bent rods with a planar curve designed for idiopathic scoliosis cannot be used for the surgery of adult spinal deformity, shown in Fig. 1(c).

This paper proposes a method to identify an optimal set of standardized pre-bent rod shapes for correction surgeries of adult spinal deformity. For this purpose, we extract rods' center points from the existing rod shapes using a CT scan, analyze the three-dimensional similarity between their center curves, and derive an optimal set of standardized pre-bent rod shapes having spatial curves.

### Method of Shape Similarity Analysis and Standardization of Pre-bent Rods:

#### Outline and Range of Analysis

Fig. 2 shows the outline of process pipeline of the proposed method. The method consists of (1) CT scan of existing spinal rods used in past corrective surgeries, (2) extraction of rods' center points from CT scan by mesh processing, (3) shape similarity evaluation of rod center point sets using Iterative Closest Points (ICP) [2], (4) grouping of similar-shaped rod center points through hierarchical cluster analysis to identify the number of the pre-bent rods, (5) derivation of the center curves of each standardized pre-bent rod by least-square fitting of a B-spline curve with similar-shaped center points, and (6) generation of surfaces of standardized rods. Details of the processes will be described in the following sections, from section 2.2 to 2.5.

As shown in Fig. 3, the shapes of spinal rods for adult spinal deformity correction exhibit moderate difference among patients in the interval from sacrum to the lumbar spine and to the thoracic spine T10. Most rod breakage due to intraoperative bending also occurs within this interval. On the other hand, the similarity among the rods becomes significantly low in patients from the distal part of the center of their thoracic spine. And it is not easy to standardize the rod shape in the distal part. Moreover, rod breakage rarely occurs in the distal part. For these reasons, the similarity evaluation and standardization of rod shapes were limited to the evaluation interval  $I_e$  between the sacrum and thoracic spine T10, as shown in Fig. 3. In addition, since the reference point at the time of surgery is always taken at the rod's fixation point to the sacrum, we place the starting point of interval  $I_e$  at the fixation point and evaluate the similarity between existing rod shapes so that the starting point of  $I_e$  always coincides.

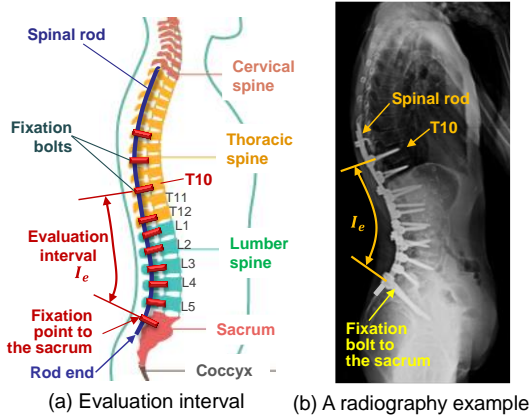


Fig. 3: Range of similarity analysis of spinal rods.

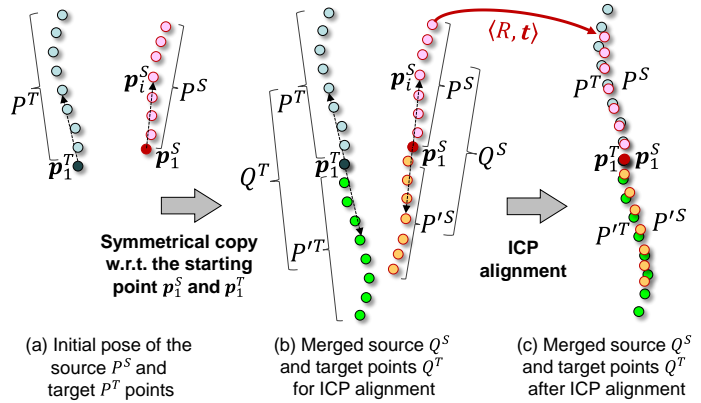


Fig. 4: Shape similarity evaluation between the center points of two rods.

### CT scan of Existing Spinal Rods and Extraction of Rod Center Points

The spinal rod for adult spinal deformity correction often exhibits a spatial curve shape, and the measurement of the existing rod shape cannot be performed by manual tracing. Therefore, in our method, the rods have been measured three-dimensionally with a medical CT (image resolution  $512 \times 512$  pixels) immediately after being bent during surgery. Then, the rod surface  $M_a^i$  represented by a triangular mesh is extracted from CT volume data as the isosurface.

Next, to stabilize the extraction of rod center points from the rod surface,  $M_a^i$  is first re-meshed using isotropic explicit remeshing [1] to generate a simplified mesh  $M_b^i$  with an edge length of about 1 mm. Then, iterative mesh contraction and topological simplification [5] are applied to  $M_b^i$  to derive a point cloud  $P_b^i$  on the medial axis of  $M_b^i$ . The points in the point cloud  $P_b^i$  are treated as center points of rod  $i$ .

### Shape Similarity Evaluation for Rod Center Points

Next, shape similarity in evaluation interval  $I_e$  is evaluated for center points of all existing rods. To this end, best fit alignment is first performed by ICP [2] between every pair of center points  $\langle P_b^i, P_b^j \rangle$  of rod  $i (\in R)$  and  $j (\in R)$  included in the CT-scanned rod set  $R$ . However, the original ICP allows centroids of  $P_b^i$  and  $P_b^j$  to align, and the fixation points to the sacrum of  $P_b^i$  and  $P_b^j$  do not coincide after the alignment. To avoid this, we have modified the ICP-based alignment so that the fixation points on rod  $i$  and  $j$ , which are the starting points of evaluation intervals  $I_e^i$  and  $I_e^j$ , are perfectly matched. The evaluation interval  $I_e$  on each rod is determined by manually measuring the positions of fixing bolts on the sacrum and thoracic spine T10 from the patient's radio graph after the surgery.

The proposed best fit alignment is performed as shown in Fig. 4. First, the subsets of center points included in the evaluation intervals  $I_e^i$  and  $I_e^j$  are extracted as  $P_e^i$  and  $P_e^j$  from  $P_b^i$  and  $P_b^j$ . The points  $p_1^i \in P_e^i$ ,  $p_1^j \in P_e^j$  closest to the fixation points to their sacrum are selected as the starting points of  $P_e^i$  and  $P_e^j$ . Next, as shown in Fig. 4(a), of  $P_e^i$  and  $P_e^j$ , the ones with longer chord length are chosen as target points  $P^T = \{p_1^T, \dots, p_M^T\}$ , and the ones with shorter chord length are chosen as source points  $P^S = \{p_1^S, \dots, p_N^S\}$ . Then, as shown in Fig. 4(b), the points  $P^T$  and  $P^S$  are symmetrically copied with respect to their starting points  $p_1^T$  and  $p_1^S$  to obtain the symmetric points  $P'^T$  and  $P'^S$ , and merged target and source points  $Q^T = P^T \cup P'^T$  and  $Q^S = P^S \cup P'^S$  are created. Then, the merged source points  $Q^S$  are best fitted with the merged target points  $Q^T$  using ICP. Because the centroids of both merged points  $Q^T$  and  $Q^S$  are starting points  $p_1^T$  and  $p_1^S$ , this modified ICP algorithm can find the best fit alignment between the source and target points  $P^T$  and  $P^S$  so that their starting points  $p_1^T$  and  $p_1^S$  are perfectly matched, shown in Fig. 4(c). Finally, the optimum transformation  $\langle R, t \rangle$  for the merged source points  $Q^S$  is

obtained from this best fit alignment, and we evaluate the RMS fit error  $D_{rms}^{i,j}$  between  $P_e^i$  and  $P_e^j$  in the evaluation intervals  $I_e^i$  and  $I_e^j$  from Eqn. (1).

$$D_{rms}^{i,j} = \sqrt{\frac{1}{|P^S|} \sum_{p_k^S \in P^S} \|R p_k^S + \mathbf{t} - \mathbf{p}_{c(k)}^T\|^2} \quad (1)$$

where  $\mathbf{p}_{c(i)}^T$  is the point in target points  $P^T$  that is closest to  $\mathbf{p}_i^S$  after best fit. Finally, we adopt  $D_{rms}^{i,j}$  as a measure of “shape dissimilarity” between the center points of rod  $i$  and  $j$ , and the dissimilarity evaluations are performed for all pairs of different rods  $(i, j)$  ( $i, j \in R$ ) in the CT-scanned rod set  $R$ .

#### Grouping of Similar-shaped Rod Center Points by Hierarchical Cluster Analysis

The larger the number of standardized rods in the pre-bent rod set, the more it can be adapted to the individual differences in patients. Still, on the other hand, from the viewpoint of manufacturing cost, we should reduce the number of rods as much as possible. Therefore, we perform a hierarchical cluster analysis where the shape dissimilarity between rod pairs, evaluated in section 2.3, is used to mediate it. From the dendrogram, we can analyze the relationship between the number of clusters that equal the number of standardized rods to be designed and the maximum RMS fit error among the existing rods belonging to one cluster. Finally, we determine the appropriate rod clusters by setting an allowable RMS fit error. In the analysis, the complete-linkage clustering has been adopted as the linkage criteria.

#### Derivation of the Center Curves of Standardized Rod Shapes by the Least-Square Fitting

After the appropriate rod clusters are determined, the center curve of the standardized rod that best fits all center points of the existing rod included in a cluster is derived as a B-spline curve using least-square fitting [4] as the following process: (1) the least-squares line is fitted to the center point clouds of multiple rods included in a cluster that has been already aligned using the ICP-based best fit alignment given in section 2.3, (2) the initial values of passing parameters and knot vector at each center point are estimated from the projections of center points on this line, (3) the cubic B-spline curve's control point positions that fit all center points are estimated in the least-square manner, (4) the passing parameter values are corrected by re-projection of center points on the B-spline curve, (5) by repeating the least-square fitting and re-projection until the control point positions become stable, we can find the center curve of the standardized rod shape of a cluster that best fits the center points of similar-shaped rods as a B-spline curve. Finally, the triangle mesh of the standardized rod shape can be generated by sweeping a circle with a standardized rod radius along the B-spline curve.

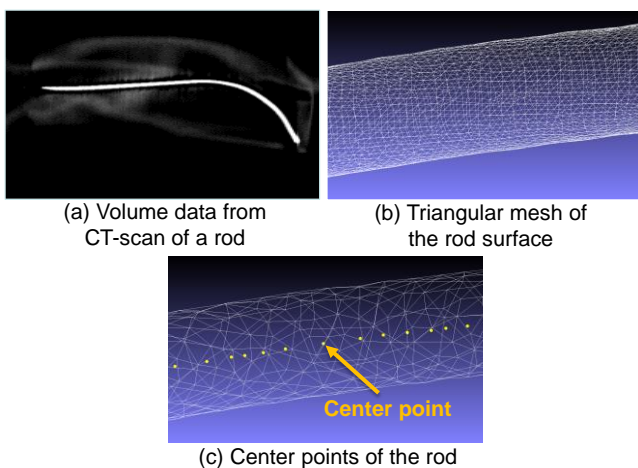


Fig. 5: An example of volume data, triangular mesh, and center points of a rod.

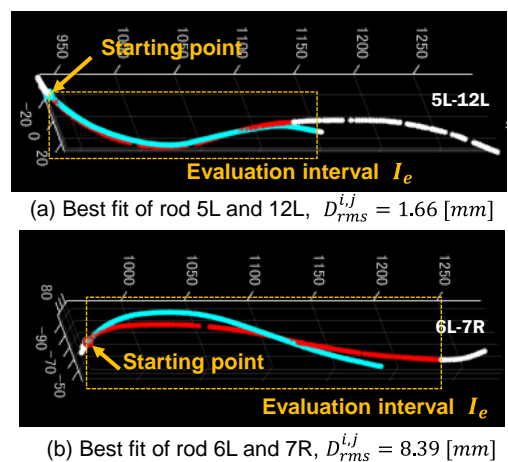


Fig. 6: Examples of shape dissimilarity evaluation between two center points.

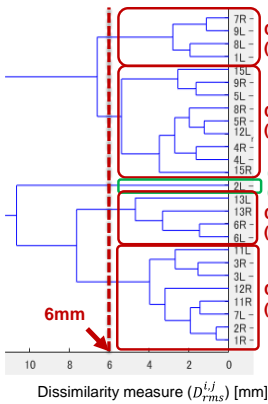


Fig. 7: Dendrogram of the cluster analysis.

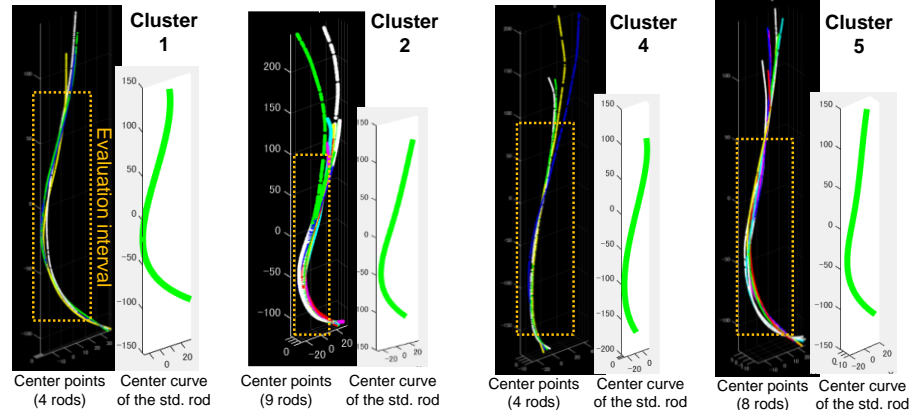


Fig. 8: Center points of each cluster and center curve of the standardized pre-bent rod for the cluster.

### Case Study:

Twenty-six left and right spinal rods for thirteen patients who underwent adult spinal deformity correction surgery at Dokkyo Medical University were measured by a medical CT-scanner, and the shape similarity estimation between these rods was performed using the proposed method. We had received informed consent from all patients before the study.

Fig. 5 shows an example of volume data from the CT scan of a rod, the triangular mesh of rod surface, and the center points of the rod. The center points of the rod can be extracted correctly. Fig. 6 shows examples of shape dissimilarity evaluation between the center points of two rods. The evaluation is only limited to the evaluation interval  $I_e$  between the sacrum, lumbar spine, and the thoracic spine T10. Fig. 6 clearly shows that the smaller the RMS fit error  $D_{rms}^{i,j}$ , the more similar the rod shapes are, and the error  $D_{rms}^{i,j}$  can work as a valid measure for evaluation of rod shape dissimilarity.

Fig. 7 shows a dendrogram of the hierarchical cluster analysis of 26 rod shapes using  $D_{rms}^{i,j}$  as the dissimilarity measure. From this figure, many cases can be seen wherein the left and right rod shapes of different patients are highly similar, and it is considered that the pre-bent rods can be designed without distinguishing between the left and right rods. In the dendrogram, when the allowable RMS fit error among the existing rod shapes in one cluster was set to 6 mm, which is the tolerance allowed in normal surgery, five rod clusters were derived, shown in Fig. 7.

Of these, we estimated that the rod shapes contained in four clusters (clusters 1, 2, 4, and 5), including four or more rods, are highly versatile, and standardized pre-bent rods must be designed for these clusters. Meanwhile, the rod in cluster 3, which contains only one rod, seems to have a peculiar shape, and since it is used infrequently, the need to design a pre-bent rod is low.

Finally, we have derived the center curves of the four standardized rods corresponding to clusters 1, 2, 4, and 5 within the evaluation interval  $I_e$ . Fig. 8 shows the center points included in each cluster and the center curve of the standardized rod for the cluster. We also asked an orthodontic surgeon to evaluate the curves of four standardized rods shown in Fig. 8. The surgeon answered that the four curves could reproduce the rod curvature patterns frequently used in corrective surgery of adult spinal deformity.

### Conclusions:

A method has been proposed in this work to identify an optimal set of standardized pre-bent rods for correction surgeries of adult spinal deformity. The similarity evaluation for existing rod shapes and the derivation of standardized rod shapes have been described for this purpose. The principle of proposed

method has been verified using 26 existing rod measurements taken from thirteen patients. Of course, it should be noted that more existing rod shapes need to be analyzed to determine and productize the optimal set of pre-bent rods in the future. However, the method proposed here is applicable without loss of generality.

References:

- [1] Alliez, P.; de Verdire, E.-C.; Devillers, O.; Isenburg, M.: Isotropic surface remeshing, Proc. 2003 Shape Modeling International, 2003, 49-58. <https://doi.org/10.1109/SMI.2003.1199601>
- [2] Besl, P.-J.; McKay, N.-D.: A method for registration of 3-D shapes, IEEE Transactions on Pattern Analysis and Machine Intelligence, 14(2), 1992, 239-256. <https://doi.org/10.1109/34.121791>
- [3] Kokabu, T.; Kanai, S.; Abe, Y.; Iwasaki, N.; Sudo, H.: Identification of optimized rod shapes to guide anatomical spinal reconstruction for adolescent thoracic idiopathic scoliosis, Journal of Orthopaedic Research, 36(12), 2018, 3219-3224. <https://doi.org/10.1002/jor.24118>
- [4] Plass, M; Stone, M.: Curve-fitting with piecewise parametric cubics, SIGGRAPH Comput. Graph., 17(3), 1983, 229-239. <https://doi.org/10.1145/964967.801153>
- [5] Tagliasacchi, A.; Alhashim, I.; Olson, M.; Zhang, H.: Mean curvature skeletons, Computer Graphics Forum, 31, 2012, 1735-1744. <https://doi.org/10.1111/j.1467-8659.2012.03178.x>